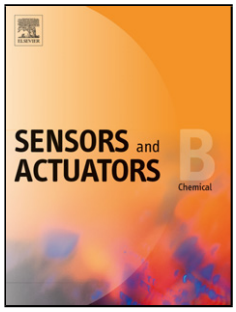
Accepted Manuscript



Title: Development of a mid-infrared nitrogen dioxide sensor based on Faraday rotation spectroscopy

Author: Kun Liu Rafał Lewicki Frank K. Tittel

PII: S0925-4005(16)31054-1
DOI: http://dx.doi.org/doi:10.1016/j.snb.2016.07.020
Reference: SNB 20518

To appear in: *Sensors and Actuators B*

Received date: 30-3-2016
Revised date: 5-7-2016
Accepted date: 5-7-2016

Please cite this article as: Kun Liu, Rafał Lewicki, Frank K.Tittel, Development of a mid-infrared nitrogen dioxide sensor based on Faraday rotation spectroscopy, Sensors and Actuators B: Chemical http://dx.doi.org/10.1016/j.snb.2016.07.020

This is a PDF file of an unedited manuscript that has been accepted for publication. As a service to our customers we are providing this early version of the manuscript. The manuscript will undergo copyediting, typesetting, and review of the resulting proof before it is published in its final form. Please note that during the production process errors may be discovered which could affect the content, and all legal disclaimers that apply to the journal pertain.

ACCEPTED MANUSCRIPT

Development of a mid-infrared nitrogen dioxide sensor based on Faraday rotation spectroscopy

Kun Liu[1,2], Rafał Lewicki[3], and Frank K. Tittel[1,✉]

[1] Department of Electrical and Computer Engineering, Rice University, Houston, Texas 77005, USA
[2] Anhui Institute of Optics & Fine Mechanics, Chinese Academy of Sciences, Hefei 230031, China
[3] Intense, North Brunswick, NJ 08902

✉ To whom correspondence should be addressed. E-mail: liukun@aiofm.ac.cn or fkt@rice.edu

Abstract: A sensitive nitrogen dioxide (NO_2) sensor system based on Faraday Rotation Spectroscopy (FRS) was developed. The advantages of FRS include high detection sensitivity, zero background and free from the influence of diamagnetic species, such as humidity and carbon dioxide. A widely tunable external cavity quantum cascade laser (EC-QCL) was used as the excitation source. The tunable EC-QCL operates mode-hop free between 1600 cm^{-1} and 1650 cm^{-1} and allows targeting the optimum $4_{41<}$-4_{40} Q-branch transition of NO_2 at 1613.2 cm^{-1} with an optical power of ~135 mW. A custom made 22.47cm long multipass gas cell (MPGC) was implemented in which the EC-QCL radiation was passed 45 times and provided an effective optical path length of 10.1 m in order to design a compact sensor system with high detection sensitivity. An air core solenoid surrounding the MPGC was used for generating a magnetic field of 200 Gauss. Performance details of a FRS based sensor and its application for long time continuous NO_2 measurements are reported. The long time stability of the sensor system was evaluated. A NO_2 detection sensitivity based on an Allan deviation plot of ~95 ppt was obtained by averaging the associated data for 300 seconds.

Key words: nitrogen dioxide detection**,** mid-infrared external cavity quantum cascade laser, Faraday rotation spectroscopy

1 Introduction

Atmospheric pollution has become a serious issue as a result of the recent population growth and industrial development as well as an increased use of fossil fuels. Nitrogen dioxide (NO_2), like sulfur oxides, carbon dioxide, and carbon monoxide are major primary pollutants in the atmosphere. The major sources of NO_2 are mainly from fossil fuel combustion processes, such as the exhaust of motor vehicles, electric power plants and industry. NO_2 is also emitted from biomass burning events and via natural processes such as during lightning events and as the result of microbial processes in the soil [1].

ACCEPTED MANUSCRIPT

Nitrogen dioxide also contributes to human health and the environment. In addition, nitrogen dioxide plays a key role in the tropospheric chemistry reactions that produce ground level ozone (O_3), which is also an important atmospheric pollutant. Furthermore, NO_2 contributes to global climate change by interfering, both directly and indirectly, with the earth's radiation budget [2-4]. According to the 2007 Fourth Assessment Report [2], anthropogenic NOx (NO and NO_2) emissions have increased drastically since preindustrial times. Therefore, there is an increasing need for the sensitive and selective detection of NO_2 in environmental atmospheric monitoring and climate research.

Conventional methods such as chemiluminescence and wet chemical analysis are the most common methods that are widely used for measurements of ambient NO_2 concentration levels. However, these methods have certain drawbacks such as that they are slow (minutes-hours) and non selective in discriminating between NO and NO_2, particularly at low concentrations. Infrared tunable diode laser absorption spectroscopy (TDLAS) is an extremely effective tool for the detection and quantification of molecular trace gases, which offers advantages that include fast response, high sensitivity, in situ and non contact measurements [5]. There are several traditional techniques for the detection of trace gases based on laser absorption spectroscopy, such as TDLAS, photoacoustic spectroscopy (PAS), quartz enhanced photoacoustic spectroscopy QEPAS) , cavity ring down (CRD) and cavity enhanced spectroscopy (CES), which have been applied to NO_2 detection [5-12]. For highly sensitive and selective detection of atmospheric trace gases it is important to select an absorption line with high intensity and minimum interference from other molecules and especially to be free from the influence of water vapor and carbon dioxide.

There are strong absorption lines in the v_3 band of NO_2, which can achieve high sensitivity by means of TDLAS, but which is limited by interference from H_2O absorption lines. Therefore, it is difficult to obtain sensitive and selective NO_2 detection with TDLAS. However, since NO_2 is a paramagnetic molecule there is a potential method for highly selective and sensitive NO_2 detection based on Faraday rotation spectroscopy (FRS), which was first reported by G. Litfin et al. in the 1980s with a color-center laser source [13]. FRS is a useful technique for quantification of paramagnetic trace gases with significantly higher sensitivity compared to TDLAS. The three basic noise sources in absorption spectroscopy measurements are source, detector, and quantum noise. Source noise results from amplitude fluctuations of the excitation laser intensity. The high sensitivity of FRS is achieved by significantly reducing source noise [13]. FRS offers the advantage of being free from the influence of non-paramagnetic molecules, such as water and carbon dioxide. This make FRS a suitable technique

ACCEPTED MANUSCRIPT

for high selective detection of paramagnetic molecules of atmospheric gases such as NO, NO_2, O_2 and OH [14-20]. For example, Lewicki et al. reported highly sensitive NO detection at 5.33 μm by employing the FRS technique using an external cavity quantum cascade laser (EC-QCL), with a minimum detection sensitivity of 4 ppbv [18]. Zhao et al. reported sensitive OH detection at 2.8 μm using FRS [19]. In 2011 So et al. obtained a minimum detection sensitivity of 30 ppmv for O_2 detection by means of the FRS technique [20].

Faraday rotation spectroscopy exploits magnetic circular birefringence (MCB) observed in the vicinity of Zeeman split absorption lines. The transition of paramagnetic molecules (such as NO_2) will undergo Zeeman splitting and split into $\Delta M_J = +1$ and $\Delta M_J = -1$ components, when NO_2 is immersed in a longitudinal magnetic field. When linearly polarized light, which can be considered as a superposition of both RHCP and LHCP light, propagates for a distance ***L*** through paramagnetic molecules immersed in a longitudinal magnetic field, its plane of polarization will rotate with an angle of $\theta = \Delta n L \pi / \lambda$, as a result of MCB. The concentration of the targeted paramagnetic molecules is proportional to $\Delta n = n_R - n_L$, the difference between the refractive index for RHCP (n_R) and LHCP (n_L) respectively. A common approach for generating FRS signals is based on an applying an alternating magnetic field, which modulates the Zeeman splitting of the absorption lines. This produces a varying MCB and results in a modulated polarization rotation of the transmitted light. After passing through the multipass gas cell, a second polarizer transforms this polarization rotation into a modulation of the light intensity prior to reaching the detector, which is then demodulated using a phase-sensitive lock-in amplifier. More details of the FRS theory are described in Refs [13,18 -22].

FRS requires that the excitation laser is single-frequency, tunable, operates at room temperature, is mode hop free and that the output wavelength coincides with the targeted molecular absorption line. In this work, an external cavity quantum cascade laser (EC-QCL) tunable between 1600 cm^{-1} and 1650 cm^{-1} was used, which allowed targeting the optimum $4_{41} \leftarrow 4_{40}$ Q-branch of the NO_2 transition at 1613.25 cm^{-1}[14].

2 Sensor design

The FRS based NO_2 sensor platform is schematically shown in Fig. 1. This platform is an improved version of the double pass configured NO_2 FRS system that was reported in Ref. [14]. Some original results of the current sensor were also reported in ref. [15]. One major improvement (or change) was using a multipass cell to replace double pass cell in ref. [14], and a detection sensitivity of 250 ppt

ACCEPTED MANUSCRIPT

was achieved with time constant of 1s, 4 times was improved than ref. [14]. In addition, laser wave length scanning with a PID controller was used in the current version for continuous, long time field measurement without drift and fluctuations of the reported sensor system.

The optical elements were mounted on an optical breadboard (18 x 24 in. in size), which makes the sensor convenient for deployment in field measurements. The temperature of the EC-QCL was set to operate at 18℃, which required the use of a water chiller. Experimental investigation showed in Ref. [14] that the $4_{41} \leftarrow 4_{40}$ Q-branch NO_2 transition at 1613.25 cm^{-1} provides a strong FRS signal with clear fingerprint. Therefore, this transition was selected, and the tunable EC-QCL allows targeting this NO_2 transition with an optical power of ~135 mW. Fig. 2 depicts the EC-QCL output power in the spectral tuning range, including an optical power drop at ~1635 cm^{-1}, caused by a H_2O absorption line. Additional components of the NO_2 sensor system include a multipass gas cell (MPGC) and a reference cell. The reference cell was filled with a ~1% NO_2 in N_2 mixture at a pressure of 25 Torr for control of the EC-QCL frequency. The MPGC was surrounded by a 15 cm long air core solenoid for generating a magnetic field inside the MCGP. The reference cell was also surrounded by a 10 cm long solenoid. The two solenoids surrounding the MPGC and the reference cell consisted of a series resonant circuit (SRL) with a 1 μF capacitor and the resonant frequency was found to be f_m = 1971 Hz. The solenoid current was supplied by a sinusoidal wave from a function generator at a frequency, matched to f_m and amplified by a commercial audio amplifier to generate the required AC magnetic field for FRS. Fig. 3 depicts the magnetic field amplitude as a function of the solenoid current, as measured by a gauss meter (FW Bell model 5180).

The MPGC used two gold coated concave mirrors with a diameter of 2 inches and a focal length of 200 mm and maximum reflectivity of 98.4% at ~ 6 μm. The distance between two mirrors was 22.47 cm, which resulted in an effective optical pathlength of 10.1 m with 45 laser beam passes. A theoretical analysis of the FRS signal strength versus the pass number of laser beam in the cell can be found in Ref. [16], in which the maximum signal was expected with 63 passes. The photo in Fig. 1 depicts a sample pattern of beam spots on the first mirror. The MPGC was designed in such a way as to tilt the angle of each mirror and to adjust the distance between two MPGC mirrors to achieve different effective optical pathlengths.

The collimated EC-QCL beam was split by a CaF_2 wedge into 2 independent optical paths. The main path propagated through the MPGC and with 45 passes. The MPGC was placed between 2 nearly crossed MgF_2 Rochon polarizers with an extinction ratio of < 10^{-5}. The first polarizer was used to

ACCEPTED MANUSCRIPT

maintain the incident beam polarized horizontally whereas the second polarizer oriented at an ~ 90 crossed position with respect to the first polarizer is used to measure the rotation of the polarization axis caused by the presence of NO_2 molecules. The optical power after the first polarizer was measured to be 84 mW and decreased to 41 mW after passing 45 times inside the MPGC. The Faraday rotated light passing through a second polarizer and was detected by a mid-infrared thermoelectrically cooled mercury-cadmium-telluride (MCT) photodetector (Vigo, model PDI-2TE-5). The AC magnetic field results in an amplitude modulation of the transmitted light intensity which was detected by a phase sensitive lock-in amplifier at the frequency f_m. The spectrum of detected FRS signal was recorded by a personal computer connected to a National Instrument data acquisition (NI-DAQ) card. For small rotation angles, the detector signal is directly proportional to the NO_2 concentration inside the MPGC.

The second optical path was used as a reference channel for controlling the EC-QCL frequency. Initially the laser beam was transformed into circular polarization by a quarter wave plate. The beam was then directed through the reference cell filled with 1% NO_2 in N_2 at a pressure of 25 Torr. The Zeeman modulation signal resulting from magnetic circular dichroism was detected by a thermoelectrically cooled MCT photodetector and demodulated by a lock in amplifier at the second harmonic frequency, f_m. The laser wavelength was scanned by a sine wave with a frequency of 1 Hz and 500 points data were acquired for each period. The first peak position of the second harmonic was used to control the laser frequency at the desired position. In case of a frequency shift from the original position a correction signal from the LabView software based PID controller was applied to the EC-QCL piezo element.

3 Sensor Optimization

The performance of the FRS based sensor system depends on several factors, such as the amplitude of magnetic field, the pressure of sample gas and the analyzer angle. The FRS signal is proportional to the amplitude of the magnetic field. Fig. 4 shows the FRS signals as a function of amplitude of magnetic field which was acquired with a mixture of 500 ppb NO_2 in N_2. The use of a magnetic field may affect the FRS signal due to the heating of the two solenoids. A magnetic field amplitude of 200 Gauss was selected, which corresponded to a current of 5 ampere and was compatible for continuous operation (a solenoid current of up to 10 ampere was feasible for short time durations).
FRS signals with different pressures were measured for determining the optimum pressure for NO_2 detection. In these measurements, the NO_2 concentration was 100 ppb for the different pressures. The

ACCEPTED MANUSCRIPT

largest FRS signal was obtained at a pressure of 30 Torr, which was selected for NO_2 concentration measurements. The performance of a FRS sensor is sensitive to the analyzer angle and must be optimized. Based on the theory introduced in Ref [18], the power transmitted through the analyzer can be expressed as

$$P = P_0[\sin^2(\alpha) + \xi] \tag{1}$$

and the FRS signal demodulated by lock-in amplifier can be expressed as

$$S = \kappa \Delta\Phi P_0 2\alpha = a\alpha P_0 \tag{2}$$

where P_0 is the intensity of light incident at the analyzer, α is the analyzer angle with respect to its crossed position, ξ is the polarizer extinction ratio, κ is the proportionality constant including the detector response, $\Delta\Phi$ is the rotation angle of the polarization of the incident light as a result of Faraday effect and $a = 2\kappa\Delta\Phi$. For a small α, the SNR can be expressed as

$$SNR = \frac{a\alpha P_0}{\sqrt{b^2 + P_0 c^2(\alpha^2 + \xi) + P_0^2 d^2(\alpha^2 + \xi)^2}} \tag{3}$$

where *b* is detector noise equivalent power (NEP), $c\sqrt{P_0(\alpha^2 + \xi)}$ is the tranmitted quantum nose, c is a coefficient related to detector responsivity, and $P_0 d(\alpha^2 + \xi)$ is the transmitted source noise (d being the proportionality coefficient specific for the used laser source). The optimum angle α_{opt} that guarantees a maximum signal-to-noise can be determined by setting the derivative of the SNR with respect to α equal to zero, and solving for α:

$$\alpha_{opt} = [(\frac{b}{P_0 d})^2 + (\frac{c\sqrt{P_0 \xi}}{P_0 d})^2 + \xi^2]^{1/4} \tag{4}$$

For a small ξ or a small laser power P_0, the optimum system performance can be achieved when the laser noise equals the detector noise, namely:

$$\alpha_{opt} = \sqrt{\frac{b}{P_0 d}} \tag{5}$$

Details of the analysis of signal-to-noise ratio (SNR) related to the angle of analyzer are reported in references [18-20]. In the present work, a series of measurements were performed for the same gas mixture at different analyzer angles to determine the optimum α_{opt} for the optimum SNR value of the FRS system. Fig. 5 shows the results of FRS signal and SNR for different analyzer angles α, which were measured with a 100 ppb NO_2 in N_2 concentration at an optimum pressure of 30 Torr. The FRS

ACCEPTED MANUSCRIPT

signal decreases when the analyzer angle α is > 5 degrees as the EC-QCL beam will saturate the MCT detector. The maximum SNR was obtained at an angle, $\alpha = 2$ degree.

4 Sensor performance evaluation

A performance evaluation based on the linearity response after optimization of the FRS based NO_2 sensor system with respect to NO_2 concentration levels was performed. A calibrated standard gas mixture consisting of 2 ppm NO_2: N_2 was employed and diluted with pure N_2 using two MKS flow meters. One flow meter with a range from 0 to 200 ccm was used to control the flow rate of the calibrated standard gas. The other flow meter with a flow range from 0 to 1,000 ccm was used to control the flow rate of pure N_2. Fig. 6 depicts the results of the FRS signal as a function of the NO_2 concentration.

Fig. 7 (a) shows a FRS spectrum of NO_2 in ambient air that was obtained by slowly scanning the EC-QCL wavelength at a scanning rate of 2 mHz, from which a noise level of 1σ = 0.24 μV was determined. The corresponding SNR was found to be 13 and the NO_2 concentration shown in Fig. 7 (a) was determined to be 3.3 ppb based on the linearity plot shown in Fig. 6. With these parameters, a minimum detection limit of 250 ppt was obtained for a 1 s time constant. However, a longer time constant can be implemented by locking of the laser frequency to the center of NO_2 absorption line [14] in order to further improve detection sensitivity.

In the following measurements, fast scanning of the laser wavelength and data averaging with different time schemes was employed. In this case the EC-QCL laser wavelength is scanned across the selected 4_{41}<-4_{40} NO_2 transition with a frequency of 1 Hz and a time constant of 10 ms. The peak position of the 2f reference signal was continuously monitored and a correction signal from a LabView software based PID controller was applied to the EC-QCL piezo element. In this manner, data with an averaging time of 10 second, 100 second and 300 second, was acquired. As an example, Fig. 7 (b) depicts the FRS spectrum of 50 ppb NO_2 acquired without averaging, averaging of 10 second, 100 second and 300 second, respectively (note: base line offset were performed for each spectrum). The noise level decreased significantly by using this approach. The minimum detection limit for 1 second, averaged in 10, 100 and 300 seconds were found to be 2.5 ppb, 1.4 ppb, 700 ppt and 240 ppt respectively. Hence the FRS based NO_2 sensor system can detect NO_2 with a MDL of 2.5 ppb in 1 second and a MDL as low as 240 ppt by averaging for 300 seconds. The FRS sensor noise level was also evaluated based on an Allan-Werle deviation analysis shown in Fig 8 [23]. Figure 8 shows that the

ACCEPTED MANUSCRIPT

FRS sensor system allows averaging times of up to 600 seconds. Hence, the minimum detection limits can be of the order of 500 ppt, 150 ppt and 95 ppt by averaging the data for 10 seconds, 100 seconds and 300 seconds, respectively. The response time of the sensor is not a critical parameter in the case of environmental monitoring, especially, when the concentration of the targeted molecules is low and a long data averaging time is beneficial for the improved measurement accuracy and precision.

5 Application of a FRS based sensor system in atmospheric NO_2 concentration measurements

Validation measurements of the developed FRS based NO_2 sensor for field applications were performed by continuously monitoring of atmospheric NO_2 at two sites located at Rice University and University of Houston, respectively. The FRS based sensor was first operated in the Rice Laser Science Group laboratory (Space Science & Technology Bldg. Suite 104) followed with air from outside the laboratory collected via a sampling tube from outside the laboratory. The sampled outside air continuously flowed into the MPGC by pumping continuously. The continuous measurements lasted >48 hours. Several distinct peaks, of up to 600 ppb NO_2 in the air, were observed during day time, as shown in Fig. 9. During the measurement period, a mobile crane was operated outside SST 104, which resulted in sharp NO_2 absorption peaks from the exhaust of the crane engines. Hence the reported FRS based NO_2 sensor system can be useful in monitoring of NO_2 emissions from motor vehicles.

The University of Houston field measurements were carried out on the top of the Moody Tower, a ~ 60 m high building located ~5 miles from the Rice University site. At this same site, a similar campaign for measuring atmospheric ammonia (NH_3) with a photoacoustic spectroscopy technique was carried out by a RLSG team in the 2010 [24]. The FRS based sensor performed continuously unattended, real-time concentration measurements of atmospheric NO_2. The sensor was capable of remote access which enabled real-time monitoring of the sensor performance from anywhere via internet. This function was successfully demonstrated by controlling the NO_2 sensor located in Houston, TX from Hefei, China, ~10,000 miles from its location in the USA. The FRS based sensor was operated for more than one month continuously. Fig. 10(a) shows the diurnal plot of NO_2 acquired during the campaign from September 12, 2011 to October 28, 2011. The black dots in the Fig. 10(a) show the mean values of the NO_2 concentration. A diurnal plot of ozone (O_3) is shown in Fig. 10(c) for convenient analysis. Fig. 10(b) shows the total, weekday and weekend diurnal plots of the NO_2 mean value obtained during the campaign, respectively. Fig. 10(b) shows that the peak mean values of the

ACCEPTED MANUSCRIPT

NO_2 concentration occurred at 8 am clock (2 pm clock GMT) with values of 22.45 ppb (total), 23.6 ppb (weekday) and 19.35 ppb (weekend), respectively. The NO_2 absorption peak mean values at 8 am (2 pm clock GMT) on weekdays are larger than the values measured on weekends. This demonstrates that NO_2 from traffic emissions exhaust contributes to the high NO_2 concentration levels in the morning hours. Furthermore, the high NO_2 concentration values in the morning are mainly due from the atmospheric chemistry reaction in the evening [1]:

$NO + O_3 \rightarrow NO_2 + O$

$O + NO + M \rightarrow NO_2 + M$

where M represents N_2 or O_2 or a third molecule that absorbs the excess vibrational energy and thereby stabilizes the NO_2 molecule. One of the key atmospheric chemistry reaction is NO_2 photolysis. During evening hours, the rapid decrease of the NO_2 photolysis rate and the abundance of atomic oxygen lead to the conversion of NO into NO_2. Thus the total number of NO_2 molecules can increase substantially in morning hours and reach their highest values at ~ 8 am (2 pm clock GMT). After 8 am (2 pm clock GMT), with the increase of sunlight intensity, NO_2 photolysis at wavelengths of < 424 nm occurs as follows [1]

$NO_2 + h\nu \rightarrow NO + O$

$O + O_2 + M \rightarrow O_3 + M$

Hence, the NO_2 concentration decreases dramatically after 8 am (2 pm clock GMT) and the concentration of O_3 is increased correspondingly, as shown in Fig. 10(a) and Fig. 10(c). The O_3 sensor is located at the same location as the FRS sensor and the data of O_3 concentration is obtained from the TCEQ website [25].

6 **Conclusions**

A compact, sensitive NO_2 sensor based on FRS was developed. The FRS technique offers advantages such as high sensitivity, high selectivity and free from the influence of diamagnetic species. The sensitivity of the present developed FRS based NO_2 sensor was enhanced by using a compact MPGC with a 10.1 m effective optical path length. The performance of the FRS based NO_2 sensor was optimized with respect to pressure, amplitude of the applied magnetic field and the angle of the analyzer polarizer. The sensitivity of the FRS based NO_2 sensor was found to be 2.5 ppb for NO_2 detection with a 10 ms time constant. The sensitivity can be further improved to < 100 ppt by averaging for 300 s. Long term, continuous, fully automated field measurements of atmospheric NO_2 using a FRS

ACCEPTED MANUSCRIPT

based NO_2 sensor, were performed. Further improvement of the NO_2 sensor system SNR value can be achieved by using better quality polarizers, a more sensitive photodetector, and reducing electronic system noise. The FRS based NO_2 sensor developed to date can be used to measure NO_2 concentration levels relevant to environmental monitoring, atmosphere chemistry research as well as exhaust analysis of motor vehicles. The FRS based sensor has an application in atmospheric chemistry research as it offers much lower atmospheric background interference than traditional laser absorption spectroscopy.

Acknowledgments: The authors gratefully acknowledge the financial support from the National Natural Science Foundation of China (Nos. 41205120, 41475023), and A US National Science Foundation (NSF) ERC MIRTHE award, a NSF–ANR award NexCILAS, as well as grant C-0586 from the Robert Welch Foundation.

References

[1] J. H. Seinfeld and S. N. Pandis, Atmospheric Chemistry and Physics: From Air Pollution to Climate Change, John Wiley & Sons, New York, 1998.

[2] S. Solomon, D. Qin, M. Manning, Z. Chen, M. Marquis, K. B. Averyt, M. Tignor, and H. L. Miller, IPCC: Climate Change 2007: The Physical Science Basis. Contribution of Working Group I to the Fourth Assessment Report of the Intergovernmental Panel on Climate Change, Cambridge University Press, Cambridge, United Kingdom and New York, NY, USA, 2007.

[3] S. Solomon, W. Portmann, R. W. Sanders, J. S. Daniel, W. Madsen, B. Bartram, and E. G. Dutton, On the role of nitrogen dioxide in the absorption of solar radiation, J. Geophys. Res., 104, 12047–12058, 1999.

[4] A. P. Vasilkov, J. Joiner, L. Oreopoulos, J. F. Gleason, P. Veefkind, E. Bucsela, E. A. Celarier, R. J. D. Spurr, and S. Platnick, Impact of tropospheric nitrogen dioxide on the regional radiation budget, Atmos. Chem. Phys., 9, 6389–6400, 2009.

[5] R. F. Curl and F. K. Tittel, Tunable infrared laser spectroscopy, Annu. Rep. Prog. Chem., Sect. C, 98, 219–272, 2002.

[6] K. Liu, X. Guo, H. Yi, W. Chen, W. Zhang, and X. Gao, Off-beam quartz-enhanced photoacoustic spectroscopy, Opt. Lett. 34, 1594 ,200).

[7] W. Chen, A.A. Kosterev, F.K. Tittel, X. Gao, W. Zhao， H_2S trace concentration measurements using off-axis integrated cavity output spectroscopy in the near-infrared, Appl. Phys. B 90, 311–315, 2008

ACCEPTED MANUSCRIPT

[8] A. Karpf and G. N. Rao, Absorption and wavelength modulation spectroscopy of NO_2 using a tunable, external cavity continuous wave quantum cascade laser, Applied Optics, 48, 408-413, 2009

[9] M. Pushkarsky, A. Tsekoun, I. G. Dunayevskiy, R. Go, and C. K. N. Patel, Sub-parts-per-billion level detection of NO_2 using room-temperature quantum cascade lasers, PNAS, 103, 10846–10849, 2006

[10] H. Yi, K. Liu, W. Chen, T. Tan, L. Wang, and X. Gao, Application of a broadband blue laser diode to trace NO_2 detection using off-beam quartz-enhanced photoacoustic spectroscopy, Opt. Lett.36, 481, 2011.

[11] M. Bitter, S. M. Ball, I. M. Povey, and R. L. Jones, A broadband cavity ringdown spectrometer for in-situ measurements of atmospheric trace gases, Atmos. Chem. Phys., 5, 2547–2560, 2005.

[12] J. M. Langridge, S. M. Ball and R. L. Jones, A compact broadband cavity enhanced absorption spectrometer for detection of atmospheric NO_2 using light emitting diodes, Analyst 131, 916–922, 2006

[13] G. Litfin, C. R. Pollock, R. F. Curl and F. K. Tittel, Sensitivity enhancement of laser absorption spectroscopy by magnetic rotation effect, J. Chern. Phys., 72, 6602-6605, 1980.

[14] C. A. Zaugg, R. Lewicki, T. Day, R. F. Curl, F. K. Tittel,Faraday rotation spectroscopy of nitrogen dioxide based on a widely tunable external cavity quantum cascade laser, Proc. of SPIE, 7945, 794500, 2011

[15] Rafał Lewicki, Kun Liua, Timothy Day, and Frank K. Tittel, Sub-ppb detection of nitrogen dioxide with an external cavity quantum cascade laser, Proc. of SPIE Vol. 8268 82682H, 2012.

[16] Y. Wang, M. Nikodem, B. E. Brumfield, and G. Wysocki, Compact Multi-pass Cell based Faraday Rotation Spectrometer for Nitric Oxide detection, in Conference on Lasers and Electro-Optics, CW3B, 2012.

[17] G. Wysocki, R. Lewicki, X. Huang, R. F. Curl, and F. K. Tittel, Continuous Monitoring of Nitric Oxide at 5.33 μm with an EC-QCL based Faraday Rotation Spectrometer: Laboratory and Field System Performance, Proc. of SPIE, 7222, 72220M, 2009.

[18] R. Lewicki, J. H. Doty III, R. F. Curl, F. K. Tittel, and G. Wysocki, Ultrasensitive detection of nitric oxide at 5.33 μm by using external cavity quantum cascade laser-based Faraday rotation spectroscopy, PNAS, 106, 12587-12592, 2009.

[19] W. Zhao, G. Wysocki, W. Chen, E. Fertein, D. L. Coq, D. Petitprez, and W. Zhang, Sensitive and

ACCEPTED MANUSCRIPT

selective detection of OH radicals using Faraday rotation spectroscopy at 2.8 μm, Opt. Express , 19, 2493-2501, 2011.

[20] S.G. So · E. Jeng · G. Wysocki, VCSEL based Faraday rotation spectroscopy with a modulated and static magnetic field for trace molecular oxygen detection, Appl Phys B (2011) 102: 279–291

[21] H. Ganser, W. Urban and J. M. Brown, The sensitive detection of NO by Faraday modulation spectroscopy with a quantum cascade laser, MOL. Phys. 101, 545–550, 2003

[22] C. R. Mahon and C. Chackerian, Zeeman Tuning Rates for Q-Branch Transitions in the v_3 Band of NO_2, J. M. Spectros 189, 276–282, 1998.

[23] P. Werle, R. R. Mücke, F. Slemr, The Limits of Signal Averaging in Atmospheric Trace-Gas Monitoring by Tunable Diode-Laser Absorption Spectroscopy (TDLAS)， Appl. Phys. B, 57,131-139 (1993)

[24] L. Gong, R. Lewicki, R. J. Griffin, J. H. Flynn, B. L. Lefer, and F. K. Tittel, Atmospheric ammonia measurements in Houston, TX using an external-cavity quantum cascade laser-based sensor, Atmos. Chem. Phys., 11, 9721–9733, 2011

[25] http:/www.tceq.texas.gov

ACCEPTED MANUSCRIPT

Author Biographies

Kun Liu received his Ph.D. degree in optics from Anhui Institute of Optics & Fine Mechanics, Chinese Academy Sciences in 2010. 2010.10–2011.11, he worked as a post doctor in Rice University, USA. Now he is an associate professor of Anhui Institute of Optics & Fine Mechanics, Chinese Academy Sciences. His research interests include photoacoustic spectroscopy and laser spectroscopy for application in atmospheric photochemistry and environmental science.

Rafał Lewicki received his M.S. degree and Ph.D. degree in electronics from Wroclaw University of Technology, Wroclaw, Poland in 2005 and 2011, respectively. In December 2005, he joined the Laser Science Group at Rice University, Houston, Texas, as a visiting scholar, and held a postdoctoral research associate position in the Department of Electrical and Computer Engineering at Rice University in 2012. His research interest is focused on trace gas detection using laser-based spectroscopic techniques, for applications in environmental monitoring, medical diagnostics, and industrial process control. He has coauthored 16 peer-reviewed journal publications, 4 book chapters, and more than 40 conference presentations in the field of laser spectroscopy.

Frank K Tittel obtained his bachelor, master, and doctorate degrees in physics from the University of Oxford in 1955 and 1959, respectively. From 1959 to 1967, he was a Research Physicist with General Electric Research and Development Center, Schenectady, New York. Since 1967 he has been on the faculty of the Department of Electrical and Computer Engineering and Biomedical Engineering at Rice University in Houston, TX, where he currently an Endowed Chaired Professor. Current research interests include various aspects of quantum electronics, in particular laser spectroscopy and laser applications in environmental monitoring, atmospheric chemistry, industrial process control, and medical diagnostics. Dr. Tittel is a Fellow of the IEEE, Optical Society of America, the American Physical Society and SPIE.

ACCEPTED MANUSCRIPT

Figure captions

Fig. 1 Schematic of the FRS based NO_2 sensor. The photo shows the distribution of beam spots produced by a red diode alignment laser incident on one of the MPGC mirrors.

Fig. 2 EC-QCL output power as a function of its spectral tuning range.

Fig. 3 Magnetic field amplitude as function of solenoid current.

Fig. 4 FRS signal as a function of magnetic field amplitude. The NO_2 concentration used in the FRS signal measurement was 500 ppbv.

Fig. 5 FRS signal and SNR as a function of the analyzer angle, α.

Fig. 6 Linear dependence of the FRS signal as a function of the NO_2 concentration.

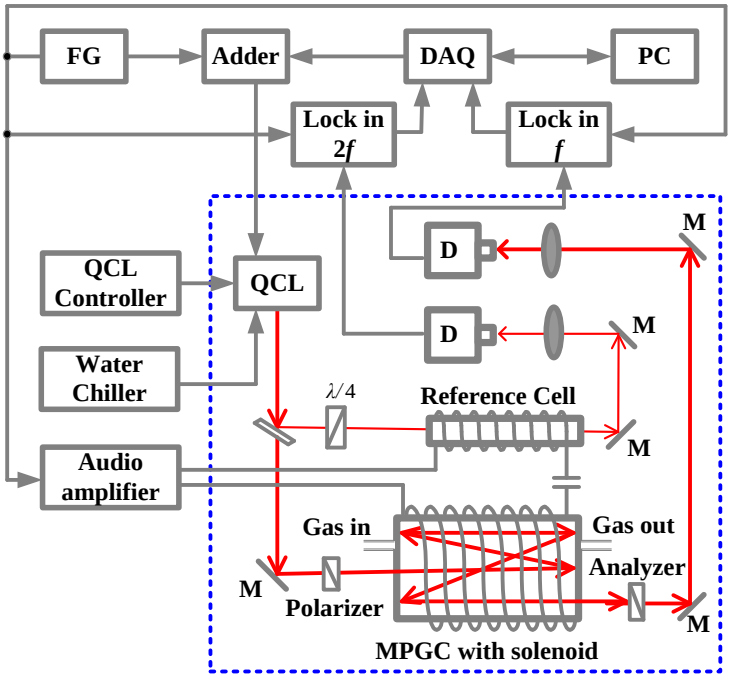
Fig. 7 FRS spectrum of NO_2 acquired in ambient air (a), and (b) FRS spectrum of NO_2 acquired from a 50 ppb NO_2 in N_2 mixture with different averaging times. Red line in Fig (a) was fitted by using 50 ppb NO_2 signal as reference.

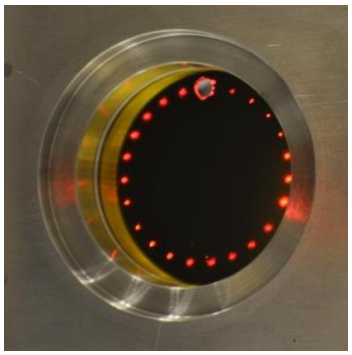
Fig. 8 Allan deviation plot of the FRS based NO_2 sensor system (bottom) and long-time, continuous measurements of 50 ppb NO_2 (top). Red line in the top represent signal averaged in 1 minute.

Fig. 9 Episode of high concentration of NO_2 observed during measurements

Fig. 10 Diurnal profiles of NO_2 (a), (b) mean values of NO_2 concentration levels during a field measurement campaign in Houston, TX from September 12, 2011 to October 28, 2011, and (c) O_3 concentrations obtained during the measurement campaign. The bottom whisker, box bottom, line inside the box, box top, and top whisker represent the 5th, 25th, 50th, 75th, and 95th percentiles of the data, and the dot inside box represent mean values in fig 10 (a) and (c), respectively.

ACCEPTED MANUSCRIPT





Red diode alignment laser beam spot pattern on one of the two MPGC mirrors

Figure 1

ACCEPTED MANUSCRIPT

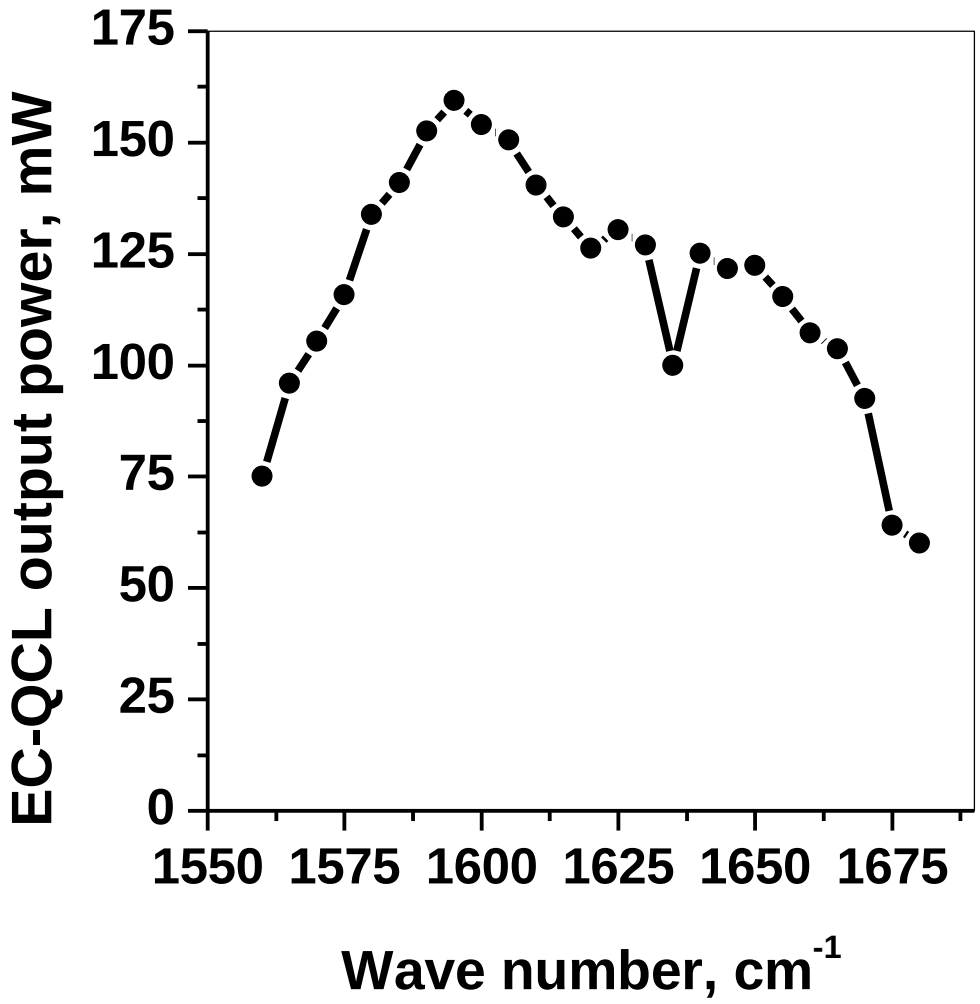


Figure 2

ACCEPTED MANUSCRIPT

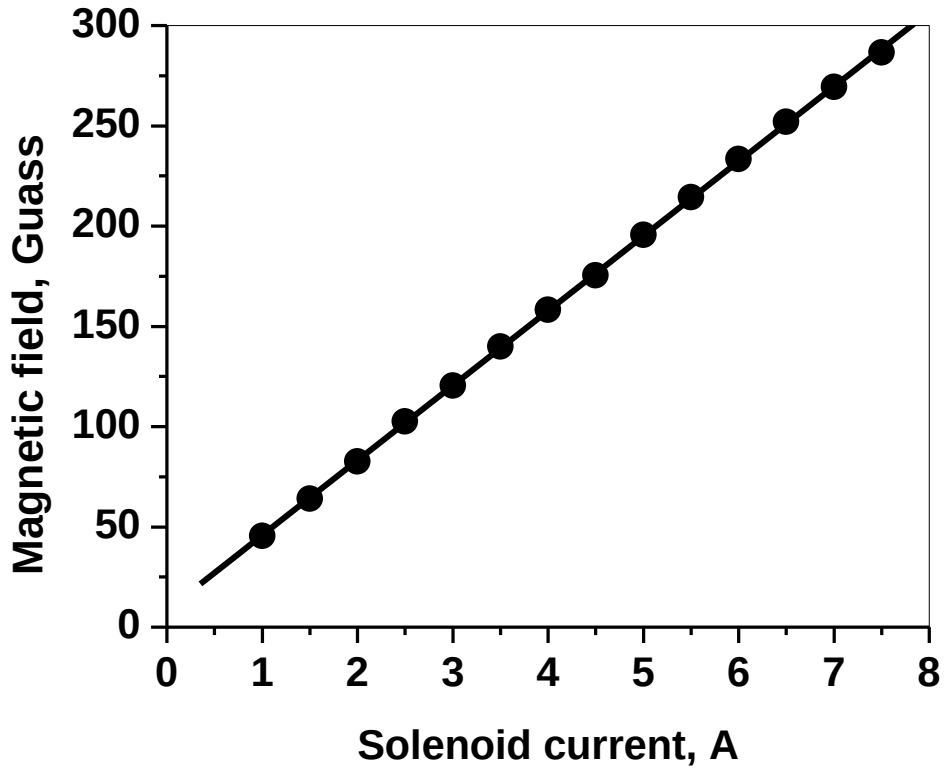


Figure 3

ACCEPTED MANUSCRIPT

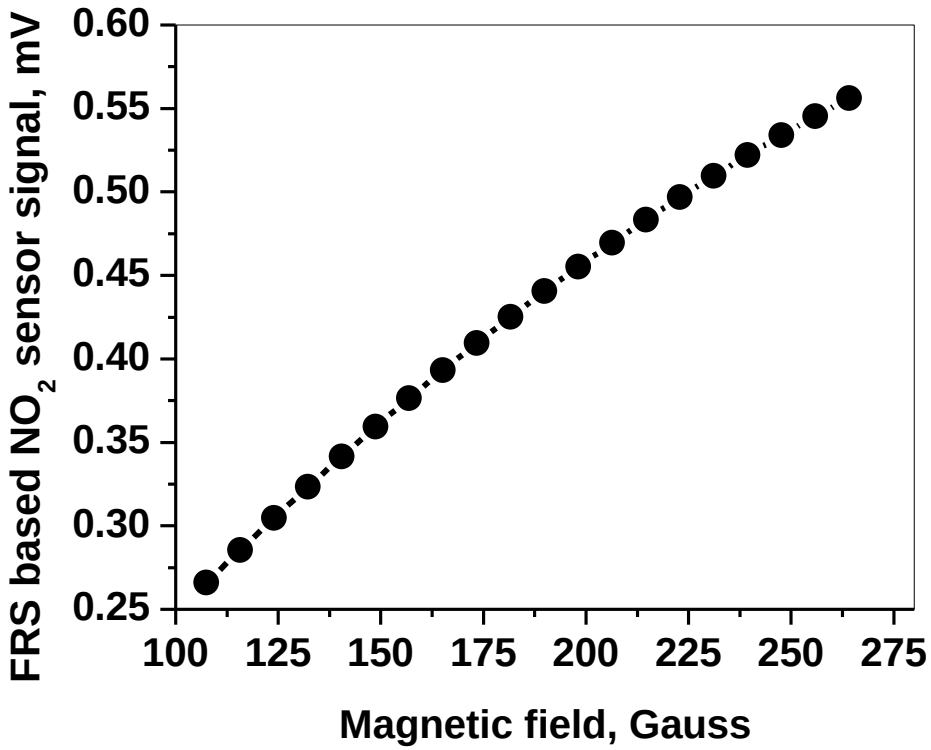


Figure 4

ACCEPTED MANUSCRIPT

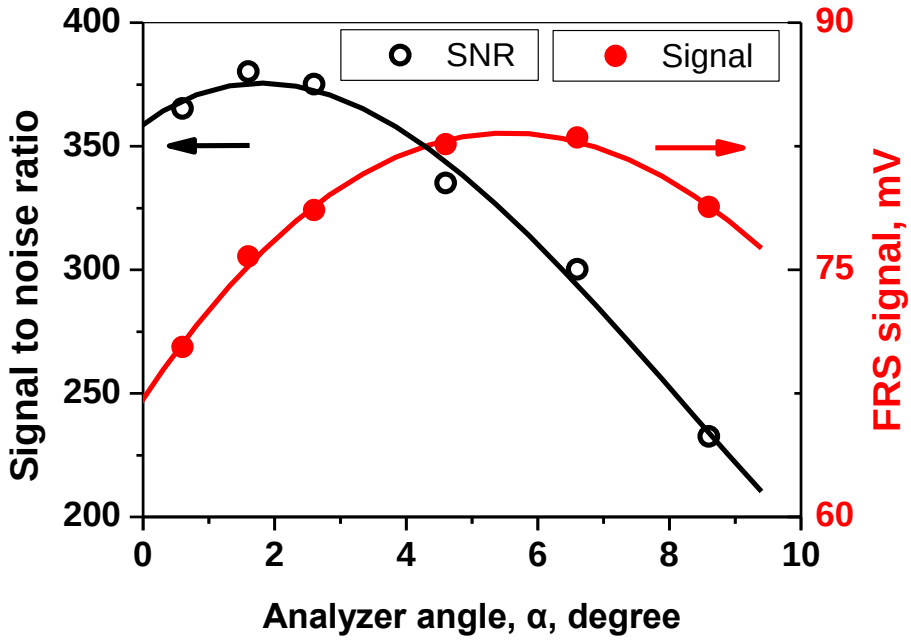


Figure 5

ACCEPTED MANUSCRIPT

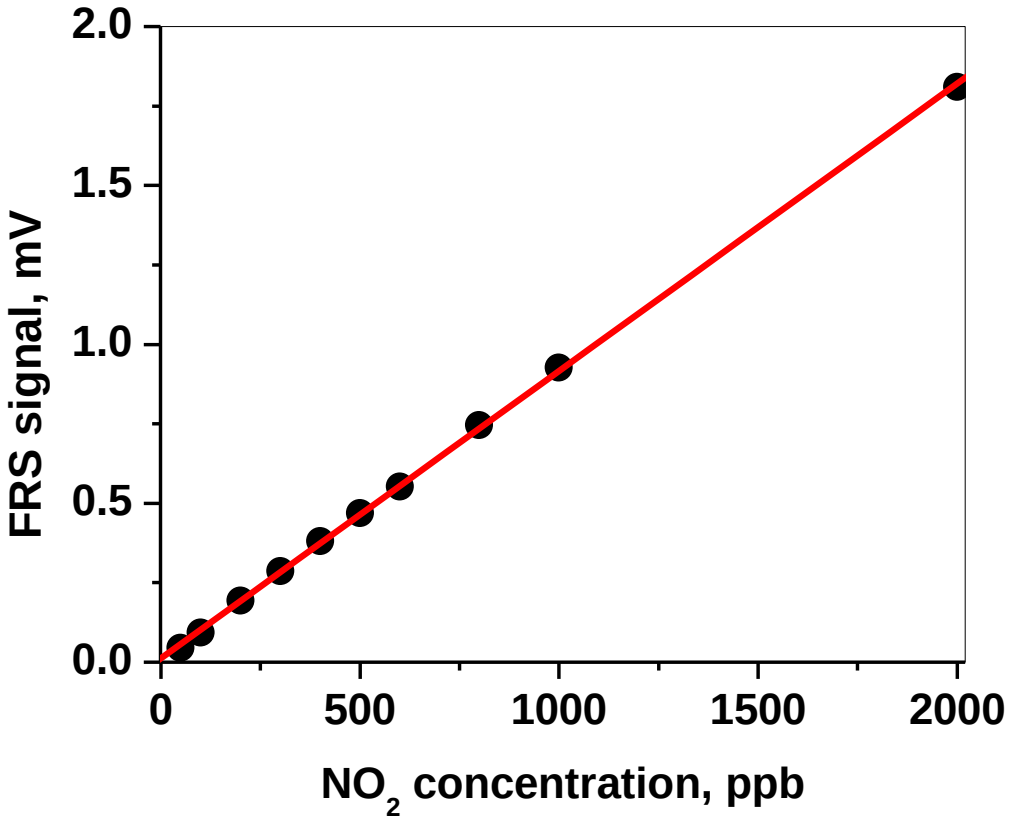


Figure 6

ACCEPTED MANUSCRIPT

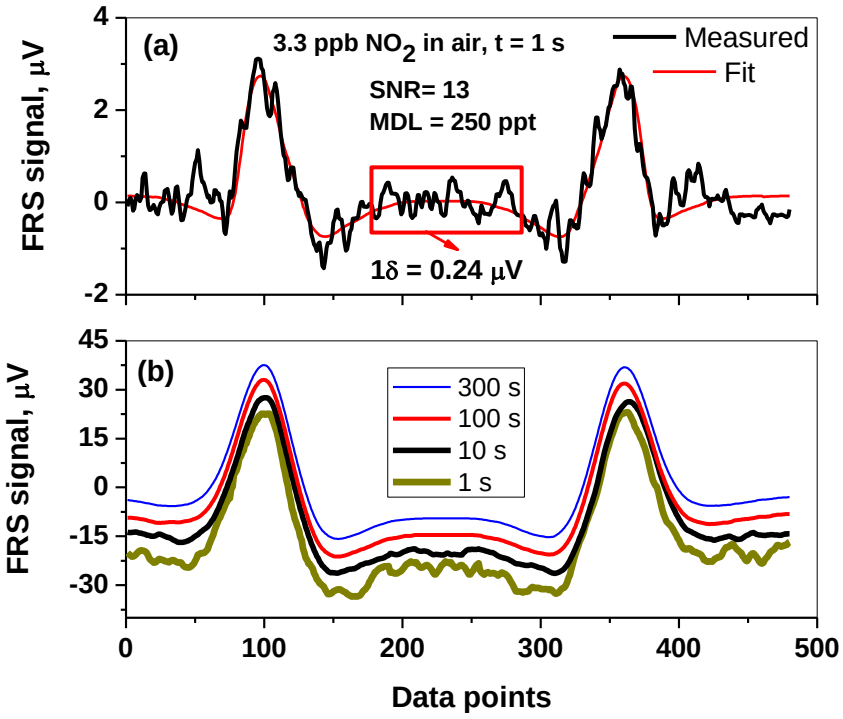


Figure 7

ACCEPTED MANUSCRIPT

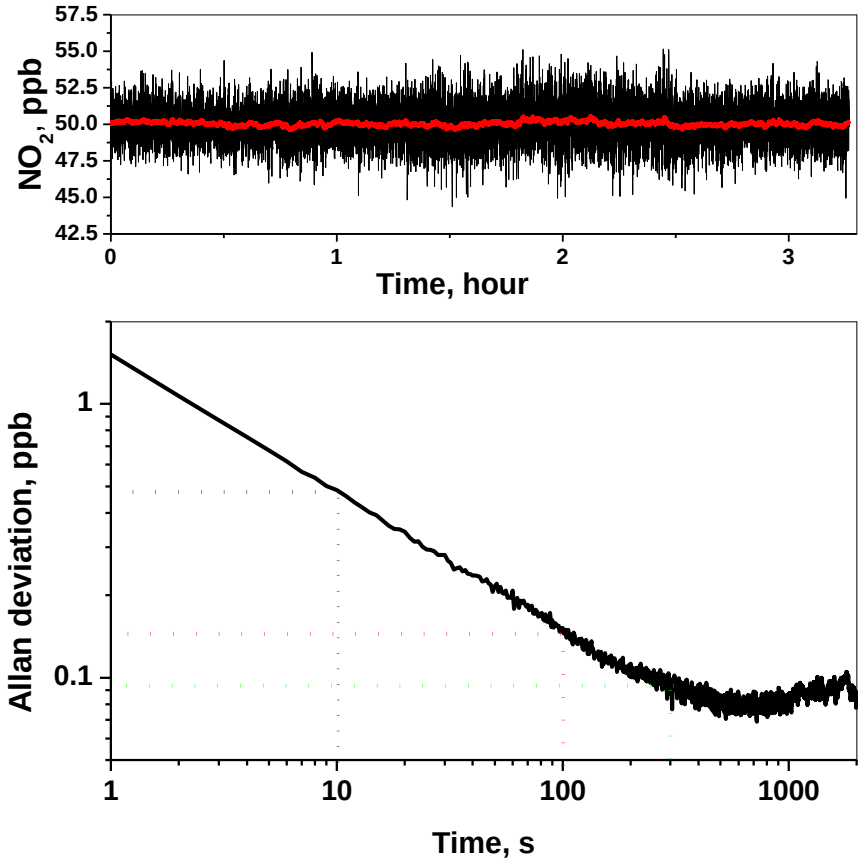


Figure 8

ACCEPTED MANUSCRIPT

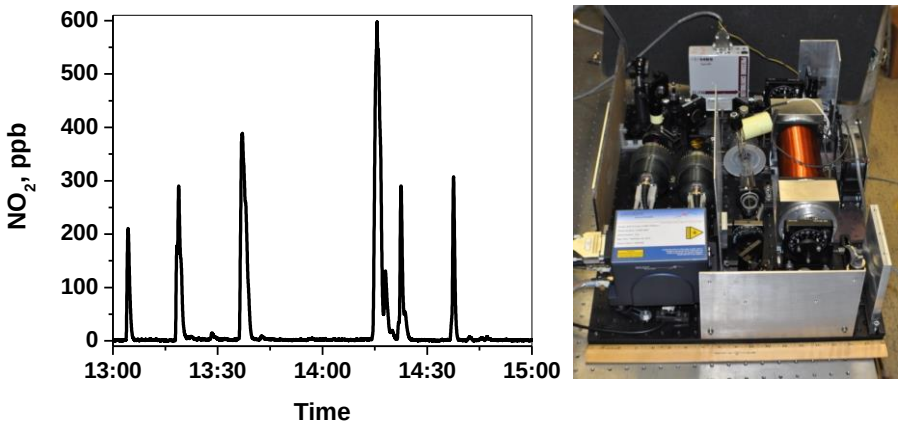


Figure 9

ACCEPTED MANUSCRIPT

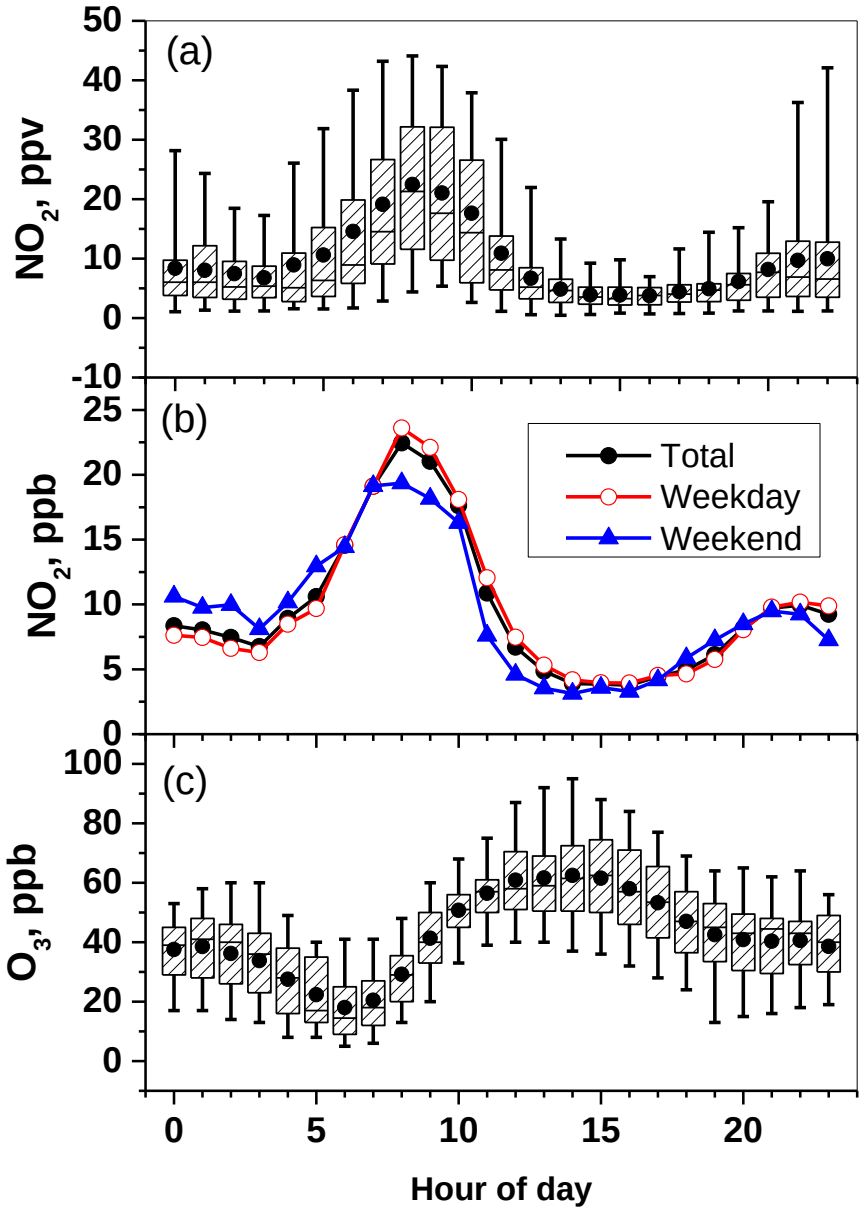


Figure 10